Communication in Physical Sciences, 2026, 13(12): 2017-2045

Integrated Remote Sensing and Aeroradiometric Data for Delineating Hydrothermal Alteration Zones and Structural Controls on Radioactive Mineralization in the Afu Younger Granite Complex, Nigeria

Abubakar Ewa Koku, and Nathaniel Goter Gok
Received: 13 August 2026/ Accepted: 29 October 2026/Published: 05 November 2026
DOI: 10.4314/cps.v13i12.10

Abstract: The Afu Younger Granite Complex, the southernmost member of the Nigerian Younger Granite province, is an A-type anorogenic complex with significant potential for rare metal and radioactive mineralization. However, detailed knowledge of the spatial distribution of its radioactive minerals and the structural control on their emplacement remains poorly constrained. This study integrates Landsat 8 Operational Land Imager (OLI) data, airborne radiometric (K, eU, eTh) surveys, and field structural analysis to delineate hydrothermal alteration zones, map radioelement distribution, and elucidate the tectonic controls on uranium (U) and thorium (Th) mineralization. Image processing techniques, including band ratios (4/2, 6/7) and Principal Component Analysis (PCA) of OLI data, were applied to map iron oxide and hydroxyl-bearing alteration minerals. The resulting mineral composite map reveals an intense, spatially extensive hydrothermal alteration system trending NE-SW. Aeroradiometric data were processed to generate individual element concentration maps and key ratios (K/Th, U/Th). The U/Th ratio map highlights zones of significant uranium enrichment (>4.5 ppm) relative to thorium, indicative of mobile uranium deposition by hydrothermal fluids. A strong spatial correlation is demonstrated between these high U/Th anomalies, the NE-SW alteration belts, and zones of high lineament density extracted from both remote sensing and aeromagnetic data. Field observations confirm the presence of pegmatite and hydrothermal quartz veins hosting cassiterite and other accessory minerals along these structures. The integration of these datasets demonstrates that a NE-SW trending structural corridor acted as the primary conduit for mineralizing fluids, controlling the distribution of hydrothermal alteration and uranium enrichment. This integrated approach effectively delineates prospective zones for radioactive mineralization and provides a robust, cost-effective model for exploration in similar granitic terrains.

Keywords: *Afu Complex, Nigerian Younger Granites, Remote Sensing, Radiometrics, Uranium Mineralization, Structural Control, A-type Granite.*

Abubakar Ewa Koku*,
Department of Mineral Resources,
Ministry of Environment and Natural Resources, Lafia, Nasarawa State.
Email: ewakoku@gmail.com
https://orcid.org/0009-0006-5819-4954

Nathaniel Goter Gok
Department of Geology and Mining
Nasarawa State University, Keffi.
Email: nathgoki@nsuk.edu.ng

1.0 Introduction

The Nigerian Younger Granite (NYG) province represents one of the world's classic examples of anorogenic alkaline ring complexes and constitutes an important geological environment for rare-metal and radioactive mineral exploration. These predominantly Jurassic intrusive complexes occur within the Precambrian Basement Complex of north-central Nigeria and are characterized by a

variety of granitic lithologies, including biotite granites, riebeckite granites, porphyritic granites and associated volcanic rocks. Their petrogenesis is associated with extensive magmatic differentiation and the development of evolved residual melts enriched in incompatible elements, including tin (Sn), niobium (Nb), tantalum (Ta), tungsten (W), lithium (Li), uranium (U) and thorium (Th) (Jacobson et al., 1958; Kinnaird et al., 1985). These characteristics have established the Nigerian Younger Granite province as an important metallogenic province with considerable potential for rare-metal and critical mineral resources (Amuda et al., 2020; Girei et al., 2019). The association between highly evolved granitic magmatism, volatile-rich residual melts and rare-metal mineralization is particularly important because magmatic fractionation and subsequent hydrothermal processes can redistribute and concentrate economically significant elements within granitic systems.

The Afu Younger Granite Complex, located in north-central Nigeria, represents the southernmost complex of the Nigerian Younger Granite province. It is composed predominantly of biotite granites and exhibits geochemical characteristics associated with advanced magmatic differentiation and post-magmatic hydrothermal alteration. Imeokparia (1981) demonstrated that the granites are enriched in volatile elements, including lithium, rubidium and fluorine, as well as ore-associated elements such as tin, tungsten, zinc and niobium. The study further established that variations in barium/rubidium (Ba/Rb) and rubidium/strontium (Rb/Sr) ratios provide useful indicators of magmatic fractionation, hydrothermal alteration and mineralization within the complex. In particular, the younger phases of the biotite granites exhibit geochemical characteristics associated with increased hydrothermal activity and mineral enrichment. Subsequent investigations have also contributed to the understanding of the petrological and geochemical evolution of the Afu Complex (Imeokparia, 1982). Its reported emplacement age of approximately 149–148 Ma further places it within the terminal stages of Jurassic Younger Granite magmatism. These geological and geochemical characteristics suggest that the complex provides a favourable environment for investigating the relationship between evolved granitic magmatism, hydrothermal fluid circulation, structural deformation and radioactive element enrichment.

Hydrothermal alteration is an important process in the development of mineralized granitic systems because circulating fluids can modify the original mineralogical and chemical composition of host rocks and redistribute metallic and radioactive elements. The interaction between hydrothermal fluids and granitic rocks may produce alteration assemblages containing iron oxides, clay minerals, sericite, chlorite, silicified zones and other secondary minerals, depending on fluid composition, temperature, pressure and host-rock chemistry. Structural features such as fractures, joints, faults and lithological contacts commonly provide pathways for fluid migration and may influence the location and distribution of mineral precipitation. In highly evolved granitic environments, these processes can contribute to the redistribution of uranium and thorium and the formation of localized mineralized zones. Consequently, understanding the spatial relationship between hydrothermal alteration, geological structures and radioelement distribution is essential for interpreting mineralization patterns and identifying prospective exploration targets.

The application of remote sensing techniques has increasingly improved the identification and delineation of hydrothermal alteration zones in mineral exploration. Multispectral satellite imagery provides spatially extensive information on surface reflectance

characteristics, allowing the identification of spectral responses associated with iron-bearing and hydroxyl-bearing minerals. Landsat imagery is particularly useful because of its relatively high spatial coverage, accessibility and suitability for regional geological investigations. Adiri et al. (2020) reviewed the application of Landsat-8 and Sentinel-2 satellite imagery in mineral exploration and demonstrated their usefulness in lithological discrimination and hydrothermal alteration mapping. Similarly, Rowan et al. (2003) demonstrated the effectiveness of multispectral remote sensing in identifying hydrothermally altered rocks through the analysis of their spectral characteristics. More recent investigations have further demonstrated the application of Landsat 8 Operational Land Imager (OLI) data and optimized band combinations for delineating hydrothermal alteration zones (Yang et al., 2024). These studies establish the importance of multispectral remote sensing as a complementary exploration technique, particularly in regions where conventional geological mapping is constrained by extensive surface cover, inaccessible terrain or limited field observations.

Among the commonly employed image-processing techniques, band ratios and Principal Component Analysis (PCA) are particularly useful for enhancing spectral differences associated with hydrothermal alteration. Band ratios emphasize variations in reflectance and absorption characteristics while reducing some effects associated with illumination and topographic variations. In Landsat 8 OLI imagery, the combination of visible, near-infrared and shortwave infrared bands can provide useful information for identifying iron oxide-bearing and hydroxyl-bearing surface materials. For example, the 4/2 band ratio can enhance the spectral response of iron oxide-bearing materials, while the 6/7 ratio can help identify hydroxyl-bearing and clay-rich alteration zones. PCA complements these techniques by transforming correlated multispectral bands into a smaller number of statistically independent components, thereby enhancing subtle spectral variations that may not be readily apparent in individual bands (Sabins, 1999; Chattoraj et al., 2020). Rowan et al. (2003) and Adiri et al. (2020) further demonstrate the relevance of multispectral image processing in mineral exploration. However, spectral anomalies identified through band ratios and PCA should be interpreted as indicators of possible alteration rather than definitive identification of specific minerals, because vegetation, weathering, soil cover and mixed surface materials can influence satellite-derived spectral responses.

Airborne gamma-ray spectrometry provides an additional geophysical approach for investigating the distribution of radioactive elements and lithological variations in granitic terrains. The technique measures naturally occurring gamma radiation associated primarily with potassium (K), equivalent uranium (eU) and equivalent thorium (eTh) in near-surface materials. These radioelements provide useful information on geological composition, weathering processes, hydrothermal alteration and mineralization (Dickson & Scott, 1997; Wilford et al., 1997). Erdi-Krausz et al. (2003) emphasized the importance of gamma-ray spectrometry in geological mapping and mineral exploration, particularly through the interpretation of individual radioelement distributions, ratios and their spatial relationships with geological features. Potassium distribution can provide information on lithological variations and hydrothermal potassic alteration, while thorium is commonly less mobile than uranium under many near-surface weathering and hydrothermal conditions. Uranium, on the other hand, can be mobilized under oxidizing conditions through the formation of soluble uranium complexes and subsequently



precipitated under favourable geochemical conditions. Consequently, variations in the eU/eTh ratio may provide useful indications of relative uranium enrichment or depletion compared with the thorium background (Dickson & Scott, 1997; Wilford et al., 1997).

The interpretation of airborne radiometric data, however, requires consideration of the geological and environmental processes that influence radioelement concentrations. Dickson and Scott (1997) demonstrated that weathering, soil formation and regolith development can significantly modify the distribution of potassium, uranium and thorium in surface materials. Similarly, Moxham et al. (1965) established that hydrothermal alteration can produce measurable changes in radioelement concentrations, particularly potassium and uranium, depending on the nature and intensity of alteration. These observations indicate that radiometric anomalies may reflect a combination of primary lithological variations, secondary alteration, weathering and mineralizing processes. Furthermore, airborne gamma-ray measurements provide information predominantly about the near-surface environment rather than the entire depth extent of underlying mineral deposits. Therefore, elevated eU concentrations or anomalous eU/eTh ratios should be interpreted as indicators of possible uranium enrichment rather than conclusive evidence of economic uranium mineralization. Their significance is better established through integration with geological mapping, structural interpretation, geochemical investigations and ground-based radiometric measurements.

The integration of remote sensing, aeroradiometric and structural datasets provides a more comprehensive approach to mineral exploration because these techniques capture complementary geological information. Remote sensing identifies surface spectral characteristics associated with alteration minerals, while airborne radiometric surveys provide information on the near-surface distribution of naturally occurring radioelements. Structural interpretation, particularly through the extraction and analysis of geological lineaments, helps identify potential pathways for hydrothermal fluid migration and zones of structural permeability. Where available, aeromagnetic data can provide additional information on subsurface geological structures, lithological boundaries and magnetic contrasts that may not be clearly expressed at the surface. The combined interpretation of these datasets can therefore improve the delineation of alteration systems and the identification of geological structures associated with potential mineralization. Studies such as Fotze et al. (2019) have demonstrated the usefulness of integrating Landsat 8 OLI/TIRS imagery with magnetic data and digital image-processing techniques for mapping hydrothermal alteration and structural features in mineralized geological environments. Such integrated approaches are particularly relevant to granitic terrains where mineralization may be spatially associated with complex intrusive relationships, hydrothermal alteration and structural discontinuities.

Despite the established rare-metal potential of the Afu Younger Granite Complex and the availability of previous petrological and geochemical investigations, important aspects of its radioactive mineralization remain insufficiently understood. Existing studies, particularly those of Imeokparia (1981, 1982), have contributed to understanding the geochemical evolution, magmatic fractionation and hydrothermal alteration of the complex. However, limited integrated information is available on the spatial relationship between hydrothermal alteration signatures, airborne radioelement distributions and geological structures within the complex. In particular, the extent to which structural lineaments influence the distribution of radiometric anomalies and

the possible concentration of uranium relative to thorium has not been adequately established through a combined remote sensing, aeroradiometric and field-based investigation. Furthermore, the individual contributions of lithological variations, hydrothermal alteration and structural controls to the observed radioelement distribution require further assessment. This limitation constrains the development of a comprehensive spatial exploration framework for identifying prospective radioactive mineralization zones within the Afu Complex. An integrated investigation is therefore necessary to bridge the gap between existing geological and geochemical knowledge and the spatial delineation of potential radioactive mineralization.

Against this background, the present study integrates Landsat 8 Operational Land Imager (OLI) data, airborne radiometric datasets comprising potassium (K), equivalent uranium (eU) and equivalent thorium (eTh), and field-based structural observations to investigate hydrothermal alteration and the structural controls on potential radioactive mineralization in the Afu Younger Granite Complex. Specifically, the study aims to: (i) delineate hydrothermal alteration zones using multispectral image-processing techniques, including band ratios and Principal Component Analysis; (ii) characterize the spatial distribution and variations of K, eU and eTh concentrations and their diagnostic ratios; (iii) evaluate the spatial relationships between radioelement anomalies, hydrothermal alteration zones and geological structures to establish their possible structural controls; and (iv) identify and delineate prospective zones of potential uranium and thorium enrichment for further geological and geochemical investigation. Where aeromagnetic data are available, their structural information is incorporated to complement the interpretation of lineaments and subsurface geological discontinuities.

The significance of this study lies in its contribution to understanding the spatial relationships between hydrothermal alteration, geological structures and radioactive element distribution within the Afu Younger Granite Complex. Scientifically, it provides an integrated framework for investigating how structural features and hydrothermal processes may influence the redistribution and concentration of radioactive elements in evolved granitic environments. Methodologically, it demonstrates the complementary application of multispectral remote sensing, airborne gamma-ray spectrometry and field structural analysis for regional mineral exploration. From an exploration perspective, the resulting alteration and radioelement anomaly maps are expected to provide preliminary information for prioritizing prospective areas for uranium, thorium and associated rare-metal investigations. The findings may also support subsequent detailed geological mapping, ground radiometric surveys, geochemical sampling and mineralogical characterization. More broadly, the integrated approach offers a potentially cost-effective exploration framework that could be adapted to comparable granitic terrains within Nigeria and other geological environments characterized by hydrothermal alteration and structurally controlled mineralization.

1.1 Geological Setting

The Nigerian Younger Granite Province

The Nigerian Younger Granite (NYG) province consists of over 50 anorogenic ring complexes intruded into the Pan-African Basement Complex of north-central Nigeria (Jacobson et al., 1958). They are Jurassic in age, with emplacement ages showing a general younging trend from north to south, ranging from ca. 213 Ma to 141 Ma (Bowden et al., 1987). The complexes are typically characterized by

circular or elliptical structures, comprising volcanic rocks (rhyolites, ignimbrites) and a wide variety of granitic rocks, including peralkaline, metaluminous, and peraluminous types (Kinnaird et al., 1985). Their anorogenic setting is linked to intraplate rifting and mantle plume activity associated with the early stages of Gondwana breakup (Burke & Dewey, 1973). Geochemically, they are classic A-type granites, enriched in alkalis, HFSEs (Zr, Nb, Y, REEs), and having high Ga/Al ratios (Whalen et al., 1987).

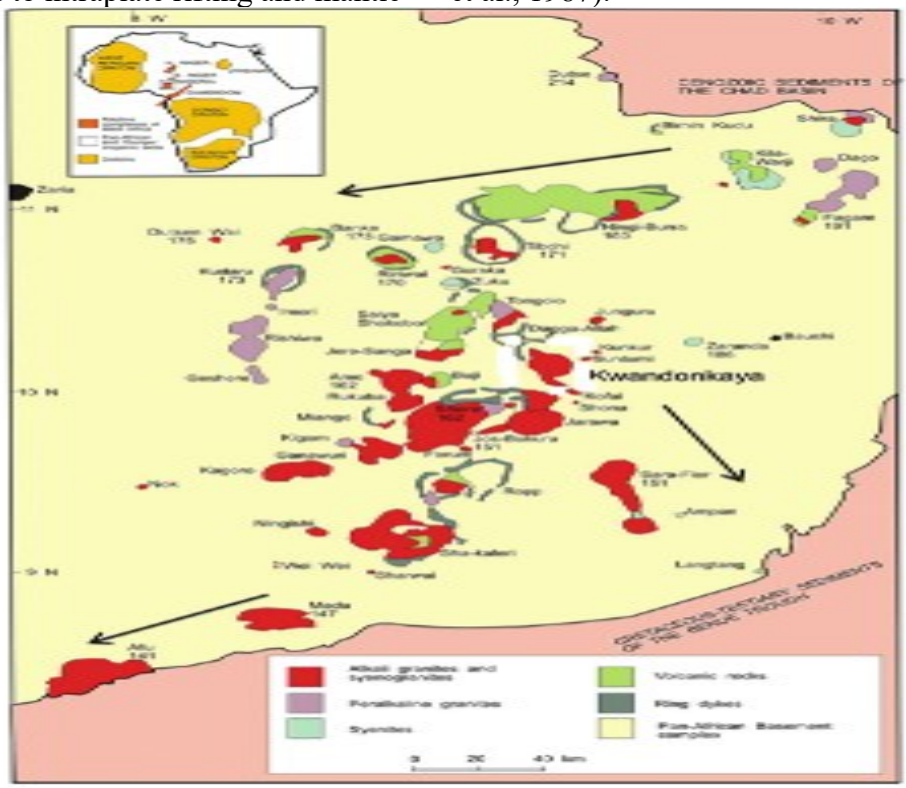

Fig. 1: Younger Granite Province of Nigeria (after Kinnard 1985) showing Afu complex

1.1 Geology of the Afu Younger Granite Complex

The Afu Younger Granite Complex (AYGC) is the southernmost and one of the youngest complexes in the NYG province, located in north-central Nigeria (Fig. 1). It is a Mesozoic anorogenic ring complex that intrudes the Precambrian Basement Complex, comprising migmatites, gneisses, and older granites. The complex is bounded to the south by Cretaceous sediments of the Benue Trough. Zircon U-Pb dating has recently constrained the crystallization age of the Afu granites to 149–148 Ma, confirming its position as marking the cessation of anorogenic magmatism in the province. The geology of the study area, a subset of the larger Afu Complex (Fig. 2), is dominated by biotite granites, which have been subdivided based on textural variations into four main units:

1. Medium-Fine Biotite Granite: This unit crops out at the southernmost parts of the area, representing the main intrusive phase.
2. Medium-Coarse Biotite Granite: This forms the most extensive sheet in the eastern, central, and part of the southwestern area, around the Odu to Agbazo region.
3. Porphyritic Biotite Granite: Occupies the north, stretching to the northwestern part of the map area, characterized by large K-feldspar phenocrysts and representing a late-stage, more evolved magma pulse.

4. Syenite Plug: A small, distinct alkaline-rich stock intrudes the porphyritic granite near its contact with the medium-coarse granite, indicating a late, highly evolved melt fraction.

These granites are typical A-type, characterized by elevated alkali oxides ($Na_2O + K_2O$ = 8.01–8.52 wt%) and high field strength elements (Zr + Nb + Ce + Y = 495–950 ppm), with a magma source dominated by crustal materials but with a contribution from mantle-derived magma. The complex is cut by a dense network of fractures, faults, and shear zones, predominantly trending NE-SW to ENE-WSW. These structures host numerous pegmatitic and hydrothermal quartz veins, some of which contain cassiterite and are associated with greisen alteration, highlighting the role of post-magmatic hydrothermal processes in metal concentration (Imeokparia, 1982).

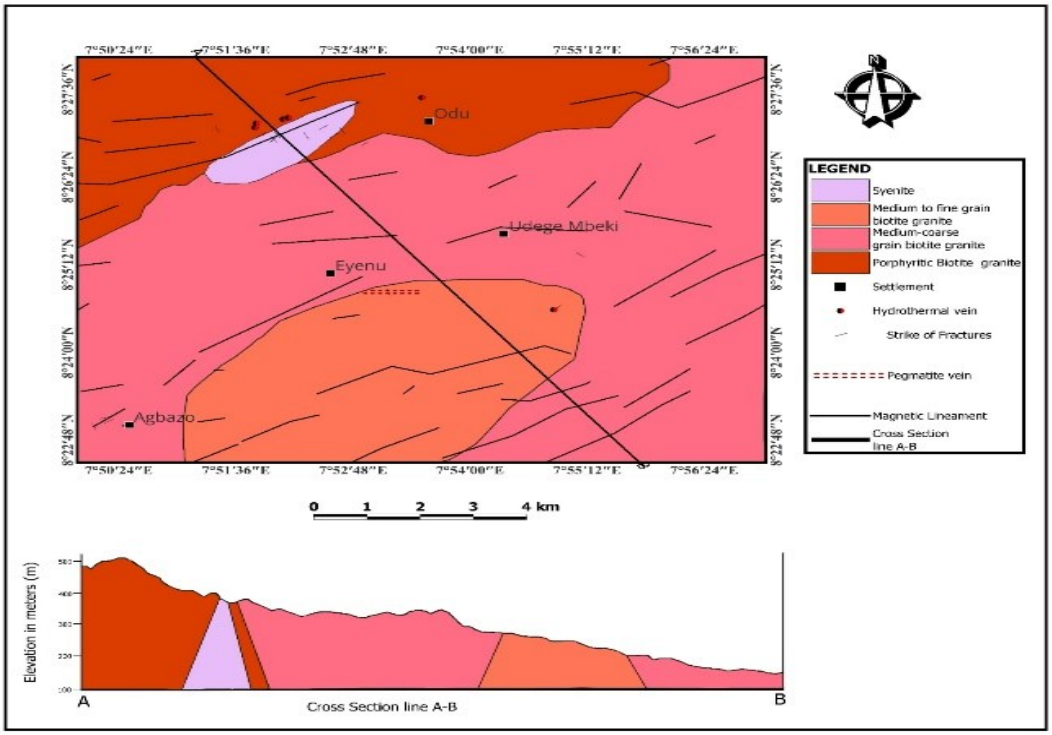

Fig. 2: Geological Map of the Study Area.

2.0 Materials and Methods

2.1 Remote Sensing Data and Processing

Landsat 8 Operational Land Imager (OLI) Level-1 data (path/row: 188/053) covering the study area were acquired from the United States Geological Survey (USGS) Earth Explorer. A cloud-free scene was selected for analysis. The data were pre-processed using ENVI software, which included radiometric calibration to convert digital numbers (DN) to top-of-atmosphere (TOA) reflectance, followed by Fast Line-of-sight Atmospheric Analysis of Hypercubes (FLAASH) atmospheric correction to derive surface reflectance values.

Several image enhancement and transformation techniques were applied:

False Colour Composites (FCCs): Various band combinations were created for visual lithological and structural interpretation. The combination RGB 752 (Band 7 (SWIR2) in red, Band 5 (NIR) in green, and Band 2 (blue) in blue) was used as it is effective for discriminating lithologies and highlighting altered zones..

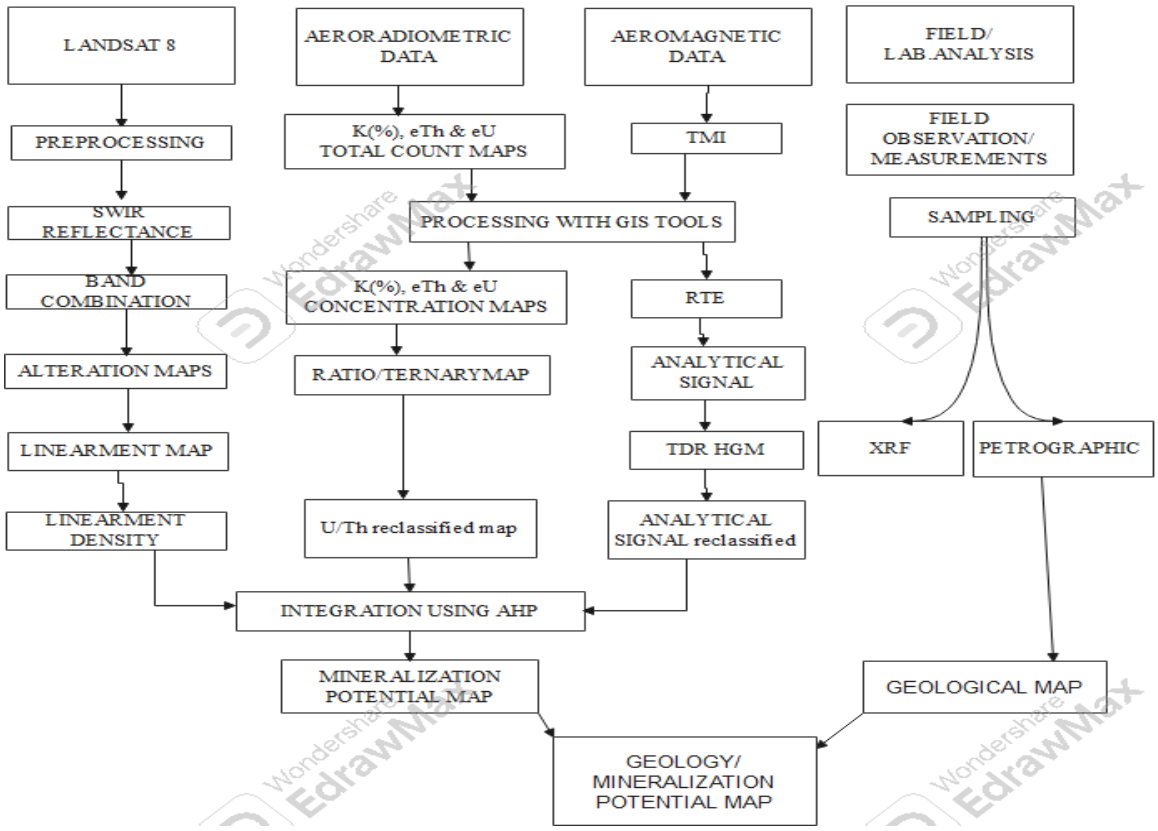

Fig.3. Methodological Flow Sheet

A methodological flowchart is presented in Fig.3. Band Ratios: To enhance specific mineral groups, band ratios were calculated. The ratio 4/2 was used to highlight iron oxides/hydroxides. The ratio 6/7 was used to \map clay and hydroxyl-bearing alteration mineralsThis study employed an integrated approach, combining satellite remote sensing, geophysical data analysis, and field verification.

Principal Component Analysis (PCA): PCA was applied to the six reflective bands (Bands 2-7) to reduce data redundancy and highlight spectral variations related to geology. The first three principal components (PC1, PC2, PC3) were combined into an RGB image to enhance lithological contrasts.

Mineral Composite Map: A colour composite image was created by assigning the hydroxyl-bearing mineral ratio (6/7) to the red channel, the iron oxide ratio (4/2) to the green channel, and a clay mineral ratio (7/6 variation) to the blue channel. This RGB image simultaneously highlights the distribution of key alteration minerals.

Lineament Extraction: Structural lineaments were visually interpreted from the PCA image and the FCCs, aided by shaded relief images derived from a digital elevation model. The extracted lineaments were used to generate a lineament density map and a rose diagram for trend analysis.

2.2 Aeroradiometric Data Processing

Airborne gamma-ray spectrometry data were acquired from the Nigerian Geological Survey Agency (NGSA). The survey was flown with a line spacing of 500 m and a terrain clearance of 80 m. The data included concentrations of potassium (K in %), equivalent uranium (eU in ppm), and equivalent thorium (eTh in ppm).

The data were processed and gridded using Oasis Montaj software. Individual concentration maps were generated for K, eU, and eTh. To enhance geological features and understand elemental mobility, several ratio maps were calculated and gridded:

K/Th ratio map: This ratio helps to highlight potassic alteration zones relative to the unaltered, Th-rich background.

U/Th ratio map: This is a critical ratio for exploration, as it highlights areas where uranium has been preferentially enriched (high ratio) or depleted (low ratio) relative to the immobile thorium.

K/U ratio map: Provides further insight into element mobility.

Ternary Map: An RGB ternary map was created by assigning K to the red channel, eTh to the green channel, and eU to the blue channel. This provides an integrated view of the relative abundance of the three radioelements, enabling rapid discrimination of different lithological and alteration units.

3.3 Field Verification

Fieldwork was conducted to verify the interpretations derived from the remote sensing and radiometric data. A total of 26 rock and soil samples were collected from locations representing different spectral and radiometric signatures, including areas of high, medium, and low anomalies (Fig. 4). Geological structures such as faults, fractures, and veins were documented, and their orientations were measured.

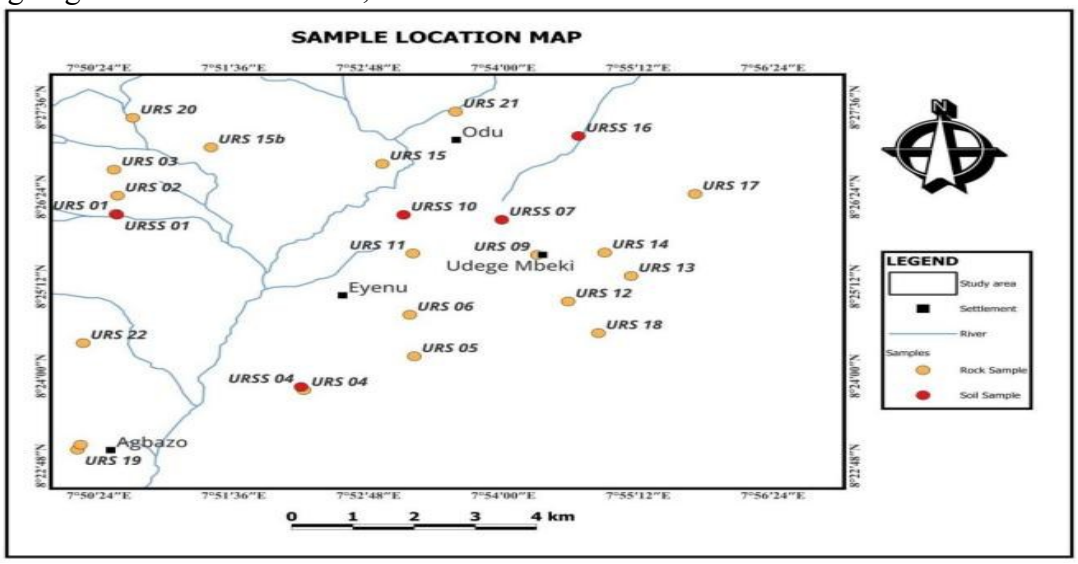

Fig.4: Sample Location Map

2.3 Geochemical Analysis

Samples collected from key lithological units were prepared and analysed for major and trace elements, including rare earth elements (REEs), using X-ray Fluorescence (XRF) at the Nigerian Raw Material Research Institute laboratory in Kaduna. The results were used to validate the lithological interpretations and to characterize the geochemical affinity of the rocks.

3.0 Results

3.1 Remote Sensing-Based Lithological Discrimination and Hydrothermal Alteration Mapping

The false colour composite (FCC) generated using Landsat 8 OLI bands 7, 5 and 2 (RGB) (Fig. 5) provides effective spectral discrimination of the major lithological units within the Afu Younger Granite Complex. The different biotite granite units exhibit

predominantly red to orange spectral responses, whereas vegetation-covered surfaces are characterized by bright green tones. The observed colour variations reflect differences in surface spectral reflectance associated with lithological composition, mineralogical characteristics and vegetation cover. A prominent NE–SW-trending linear feature is also identifiable, separating distinct lithological domains and suggesting the presence of a significant structural discontinuity. The spatial expression of this feature indicates that structural boundaries may have influenced the distribution of the intrusive units and subsequent hydrothermal alteration.

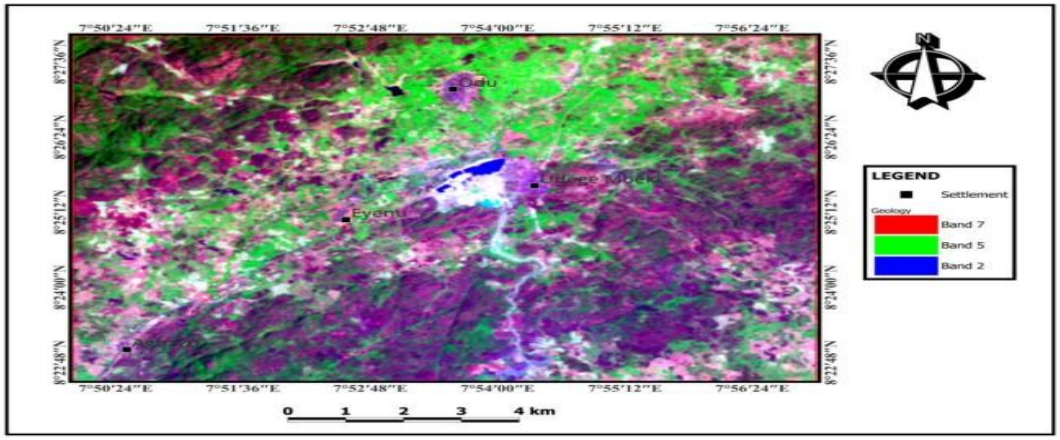

Fig.: 5. False Colour Composite map of Bands 752

The principal component analysis (PCA) composite, generated by assigning PC1, PC2 and PC3 to the red, green and blue channels, respectively (Fig. 6), further enhances the spectral differentiation of lithological units within the study area. Unlike conventional band combinations, PCA transforms correlated spectral variables into orthogonal components, thereby redistributing the spectral variance and enhancing subtle variations in surface characteristics. The resulting composite reveals lithological boundaries and spectral contrasts that are less conspicuous in the original multispectral imagery. These enhanced spectral differences provide additional information for distinguishing the various granite phases and refining the geological interpretation of the study area. The effectiveness of PCA in highlighting mineralogical and alteration-related spectral variations is consistent with the approaches described by Loughlin (1991) and Yang et al. (2024).

The mineral colour composite map (Fig. 7), derived from the integration of spectral ratios associated with hydroxyl-bearing minerals, iron oxides and clay-rich materials, provides further information on the distribution of potential hydrothermal alteration zones. The composite reveals a prominent zone characterized by magenta to pink spectral responses extending predominantly in the NE–SW direction across the central part of the study area. The spatial continuity and intensity of this spectral anomaly suggest the development of an extensive alteration zone, potentially associated with hydrothermal fluid-rock interaction along a structurally controlled corridor.

The alteration belt exhibits a close spatial correspondence with the prominent NE–SW-trending linear feature identified in the false colour composite (Fig. 5). This relationship suggests that the structural discontinuity may have provided preferential pathways for fluid migration and associated mineralogical

alteration. The coincidence of the alteration signatures with the interpreted structural trend is particularly significant because fractures and other discontinuities commonly enhance permeability and facilitate hydrothermal fluid circulation in granitic environments. Nevertheless, the mapped spectral responses represent remotely sensed alteration proxies and require field and mineralogical verification to establish the precise alteration assemblages.

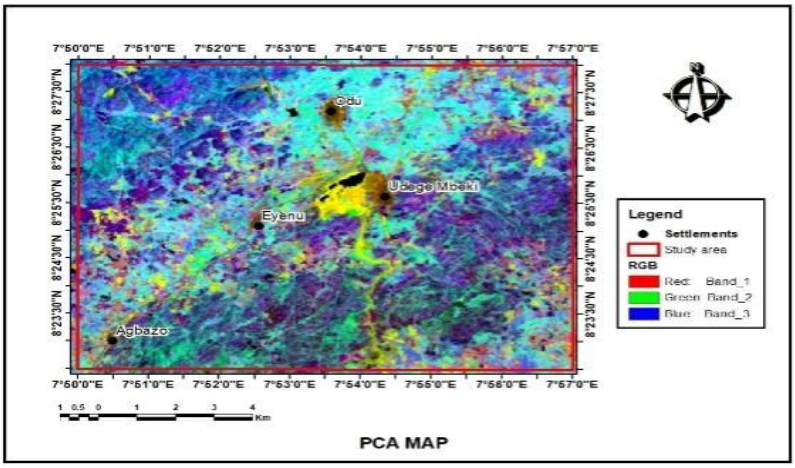

Fig. :6 PCA composite Map

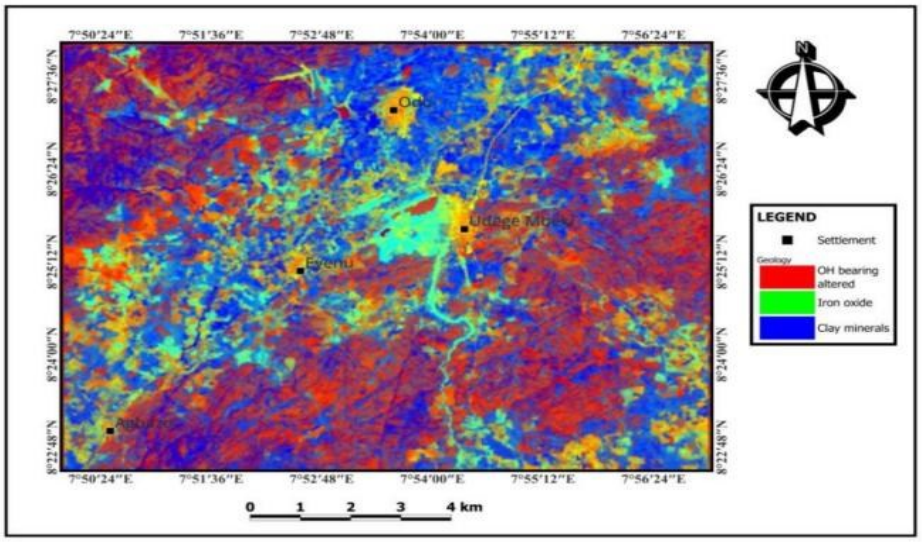

Fig: 7. Mineral Colour Composite Map

3.2 Airborne Radiometric Signatures and Radioelement Distribution

The airborne gamma-ray spectrometric data provide complementary information on the spatial distribution of potassium, equivalent uranium and equivalent thorium within the Afu Younger Granite Complex. The individual radioelement maps reveal distinct spatial variations that may reflect differences in lithological composition, accessory mineral distribution, weathering processes and possible hydrothermal alteration. Since potassium is measured directly through its gamma-ray emission, whereas uranium and thorium concentrations are estimated indirectly from their radioactive decay products, the latter are

appropriately expressed as equivalent uranium (eU) and equivalent thorium (eTh), respectively (International Atomic Energy Agency [IAEA], 2003).

3.2.1 Potassium Distribution

The potassium concentration map (Fig. 8) indicates values ranging from −0.3% to 3.6%. Elevated potassium responses, particularly those exceeding 3.1%, are represented by pink to red colour intensities and occur predominantly in the northeastern, eastern and southwestern sectors of the study area. These anomalies exhibit a broadly NE–SW-oriented distribution, suggesting a spatial association with the major lithological and structural trends identified from the satellite imagery.

The elevated potassium responses may reflect the abundance of potassium-bearing minerals, particularly K-feldspar and biotite, within the biotite granite units. In addition, localized potassium enrichment may be associated with hydrothermal alteration involving the introduction or redistribution of potassium-bearing minerals. However, the distinction between primary magmatic potassium enrichment and secondary hydrothermal potassic alteration requires supporting petrographic and geochemical evidence. Consequently, the elevated potassium anomalies are interpreted as reflecting a combination of lithological composition and possible hydrothermal modification rather than being exclusively diagnostic of potassic alteration.

The occurrence of negative potassium values, particularly the minimum value of −0.3%, also requires consideration. Since potassium concentration is physically non-negative, such values may reflect background subtraction, calibration or processing uncertainties. These values should therefore be evaluated against the original radiometric data and quality-control procedures before geological interpretation.

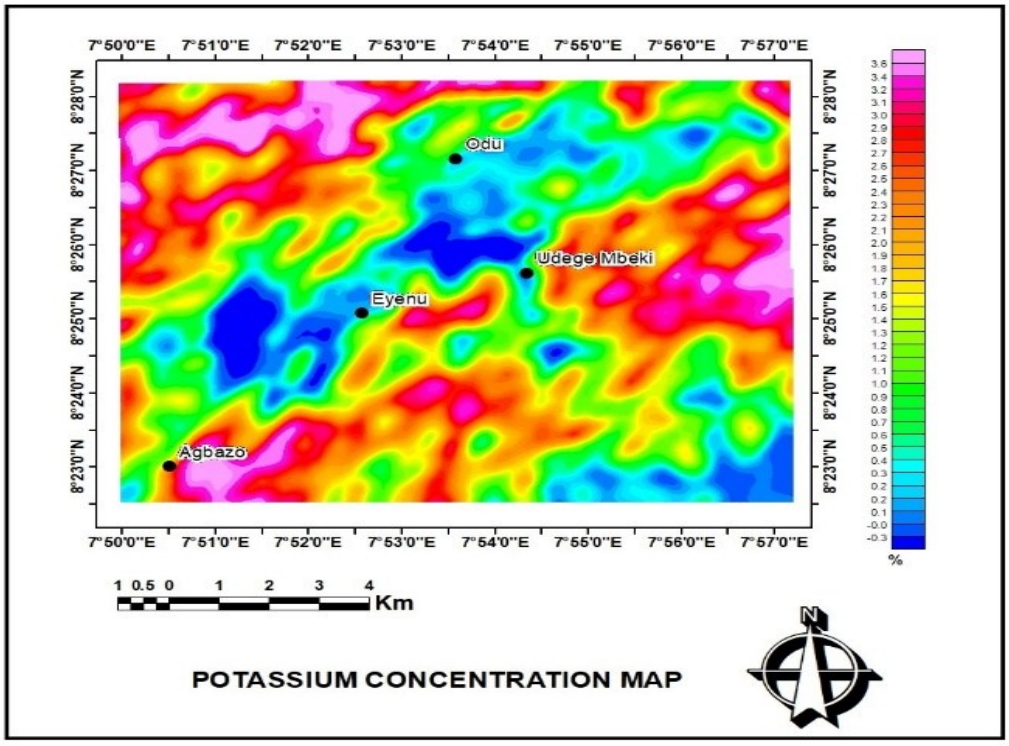

Fig. 8: Potassium concentration Map

3.2.2 Thorium Distribution

The equivalent thorium concentration map (Fig. 9) displays values ranging from 14.3 to 88.2 ppm. Relatively elevated eTh concentrations, exceeding 47.5 ppm, occur mainly in the northern, central and southeastern portions of the study area and are represented by pink colour intensities. These anomalies indicate spatial variations in the distribution of thorium-bearing minerals within the granitic units.

The observed thorium enrichment may be associated with the presence of accessory minerals such as monazite and zircon, which can accommodate significant quantities of thorium within their crystal structures. Their relative resistance to chemical weathering allows them to persist during alteration and regolith development, potentially resulting in localized thorium concentrations. In highly evolved granitic systems, the distribution of these accessory minerals may also reflect magmatic differentiation and mineralogical fractionation.

The relatively elevated eTh responses therefore provide useful information on the distribution of thorium-bearing lithological components and accessory mineral assemblages within the complex. However, distinguishing primary magmatic concentrations from secondary residual or sedimentary accumulation requires mineralogical and field-based verification.

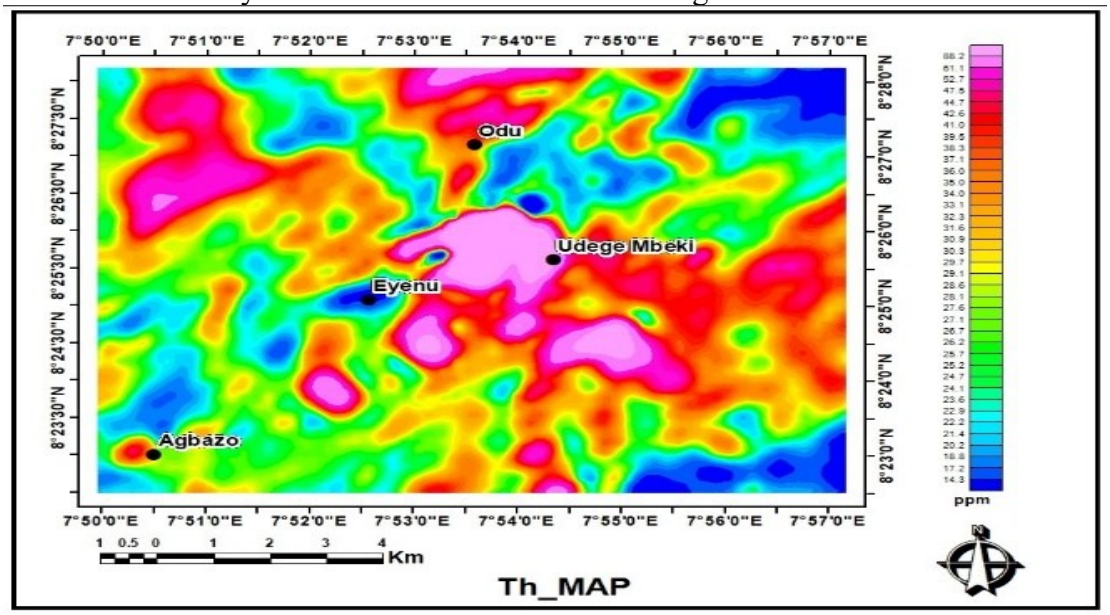

Fig.9. Thorium Concentration Map

3.2.3 Uranium Distribution

The equivalent uranium concentration map (Fig. 10) exhibits values ranging from 3.8 to 20.1 ppm. Elevated eU responses, particularly those exceeding 11.4 ppm, occur within the central, northern, northwestern and southwestern sectors of the study area. Unlike the more extensive potassium and thorium distributions, the uranium anomalies are relatively localized and occur as discrete zones of enhanced radiometric response.

The spatial distribution of these anomalies may reflect variations in the abundance of uranium-bearing minerals, differential uranium mobility during hydrothermal alteration and secondary redistribution under favourable geochemical conditions. Uranium can be transported in aqueous fluids, particularly under oxidizing conditions where soluble uranyl complexes may form, and subsequently precipitated where fluid chemistry, redox conditions or fluid-rock interaction favour uranium immobilization.

The occurrence of localized eU anomalies within the granitic complex is therefore significant for exploration because it may indicate zones of relative uranium enrichment. Nevertheless, airborne gamma-ray spectrometry estimates uranium concentration indirectly through its radioactive decay products, and disequilibrium within the uranium decay series may produce discrepancies between measured eU and actual chemical uranium concentrations (IAEA, 2003). Consequently, the identified anomalies should be treated as preliminary exploration indicators requiring independent geochemical verification.

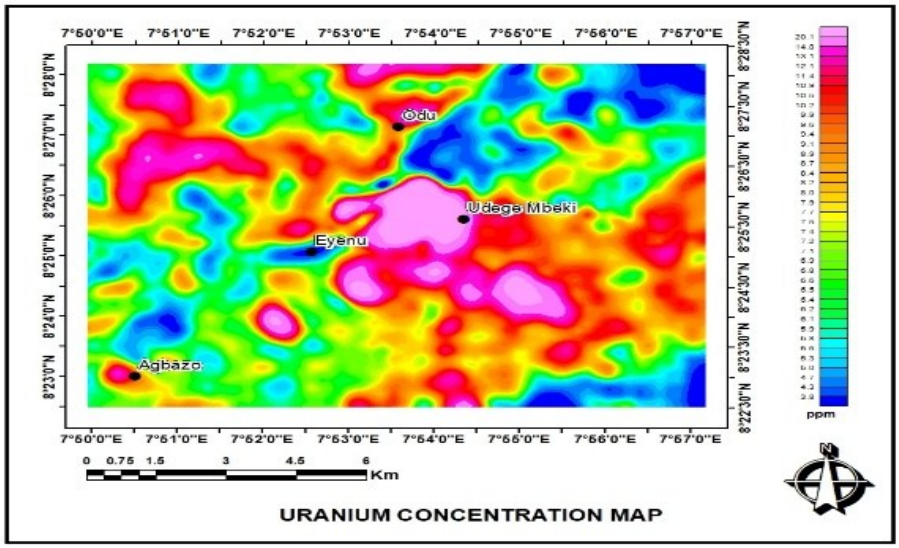

Fig:10 :Uranium concentration map

3.2.4 Potassium-to-Thorium Ratio Distribution

The K/Th ratio map (Fig. 11) provides an additional basis for evaluating variations in potassium abundance relative to the comparatively less mobile thorium component. Elevated K/Th ratios, represented by red to brown colour intensities, are concentrated predominantly along the NE–SW-trending structural corridor. This distribution broadly corresponds with the potassium-rich zones identified in Fig. 8 and the hydrothermal alteration belt delineated from Landsat 8 imagery.

The elevated ratios may indicate localized potassium enrichment relative to thorium, potentially associated with hydrothermal fluid-rock interaction and the development of potassium-bearing secondary minerals. However, elevated K/Th ratios may also arise from differences in primary lithological composition or relative depletion of thorium. Accordingly, their interpretation as evidence of potassic alteration requires corroboration from mineralogical observations, particularly the identification of secondary K-feldspar or sericite and associated alteration textures.

3.2.5 Uranium-to-Thorium Ratio Distribution

The U/Th ratio map (Fig. 12) provides an important exploration indicator for evaluating the relative enrichment of uranium compared with thorium. The map reveals localized anomalies with U/Th ratios greater than 4.5, concentrated predominantly along the central NE–SW-trending structural corridor. These anomalies coincide spatially with portions of the hydrothermal alteration belt and areas of elevated lineament density.

The observed ratio distribution suggests preferential uranium enrichment relative to

thorium within the identified structural corridor. Given the comparatively greater mobility of uranium under certain hydrothermal and oxidizing conditions, the localized increase in U/Th ratios may reflect uranium redistribution and concentration during fluid-rock interaction. The relatively immobile behaviour of thorium under many near-surface geochemical conditions makes it a useful reference element for evaluating relative uranium enrichment.

However, elevated U/Th ratios are not uniquely diagnostic of hydrothermal uranium mineralization because they may also result from uranium loss, thorium depletion, lithological variations or radioactive disequilibrium. The spatial correspondence between elevated U/Th ratios, alteration signatures and structural features therefore provides a stronger exploration indication than the ratio alone. The identified anomalies should be regarded as prospective radiometric targets rather than confirmed uranium deposits.

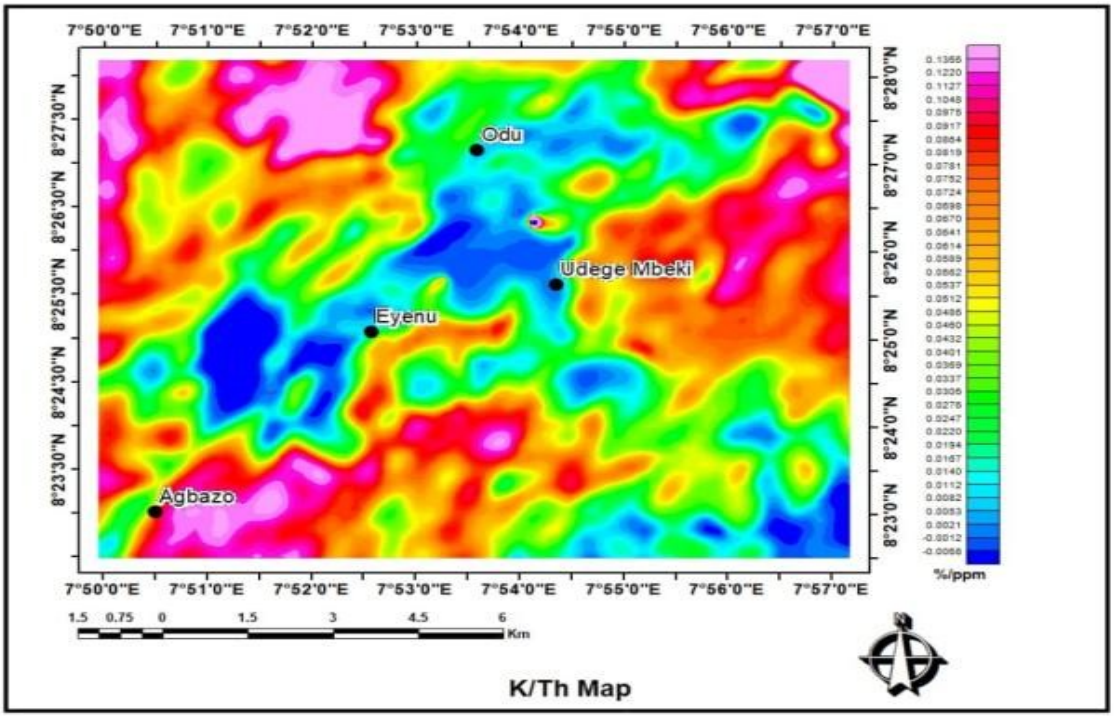

Fig.11: Potassium/Thorium map

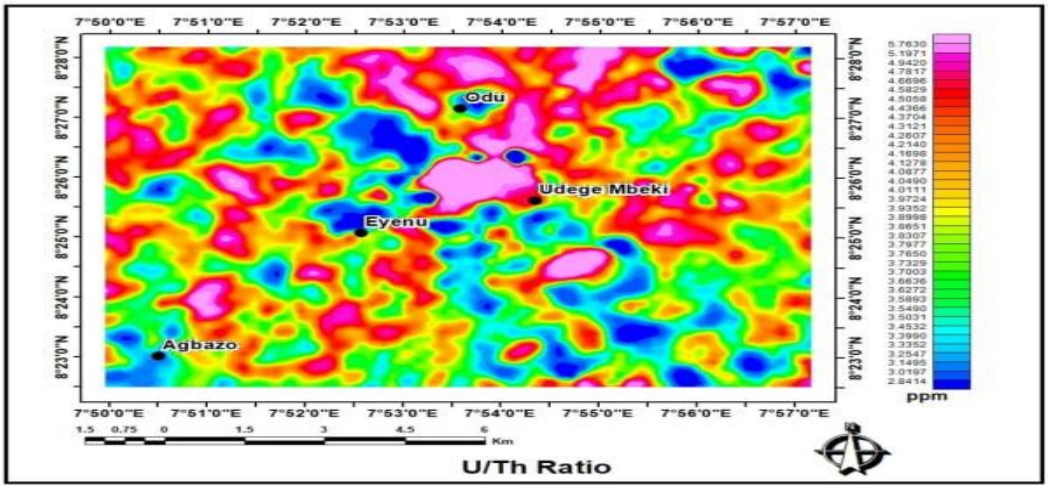

:

Fig. 12: Uranium/Thorium map

3.2.6 Radiometric Ternary Image Interpretation

3.2.6 Radiometric Ternary Image Interpretation

The ternary radiometric composite (Fig. 13), generated by assigning potassium (K), equivalent thorium (eTh) and equivalent uranium (eU) to the red, green and blue colour channels, respectively, provides an integrated visualization of radioelement distribution and their relative spatial contributions. This composite enhances the discrimination of areas with contrasting radiometric signatures and facilitates the identification of zones exhibiting distinctive lithological and geochemical characteristics.

The white to pink zones indicate areas with relatively elevated contributions from all three radioelements and are spatially associated with the porphyritic biotite granite. Their distribution may reflect the combined influence of potassium-bearing feldspars and biotite, as well as uranium- and thorium-bearing accessory minerals. The red zones are characterized by relatively high potassium contributions and may represent potassium-rich granite phases or possible zones of potassic alteration. In contrast, the blue zones indicate relatively elevated eU responses and delineate the principal uranium-related radiometric anomalies, particularly those associated with the central NE–SW structural corridor. The green zones are dominated by relatively elevated eTh responses, potentially reflecting the presence of thorium-bearing accessory minerals, including monazite and zircon, within the underlying granitic materials or residual regolith.

Overall, the ternary image integrates the individual radioelement distributions and provides a useful basis for identifying areas where contrasting geochemical signatures overlap. However, its interpretation depends on the normalization and colour-assignment procedures adopted during image generation. Consequently, the observed colour associations should be evaluated in conjunction with the individual potassium, eTh and eU distribution maps, as well as available field observations, to ensure a reliable interpretation of the radiometric characteristics and their geological significance.

3.3 Structural Framework and Lineament Analysis

The structural interpretation of the Afu Younger Granite Complex was undertaken using lineaments extracted from Landsat 8 imagery and aeromagnetic datasets. The

resulting lineament map (Fig. 14) reveals a predominant NE–SW to ENE–WSW structural orientation, accompanied by a subordinate E–W-trending structural set. These orientations indicate the presence of a dominant structural grain that may have influenced the emplacement, deformation and subsequent hydrothermal modification of the granitic complex.

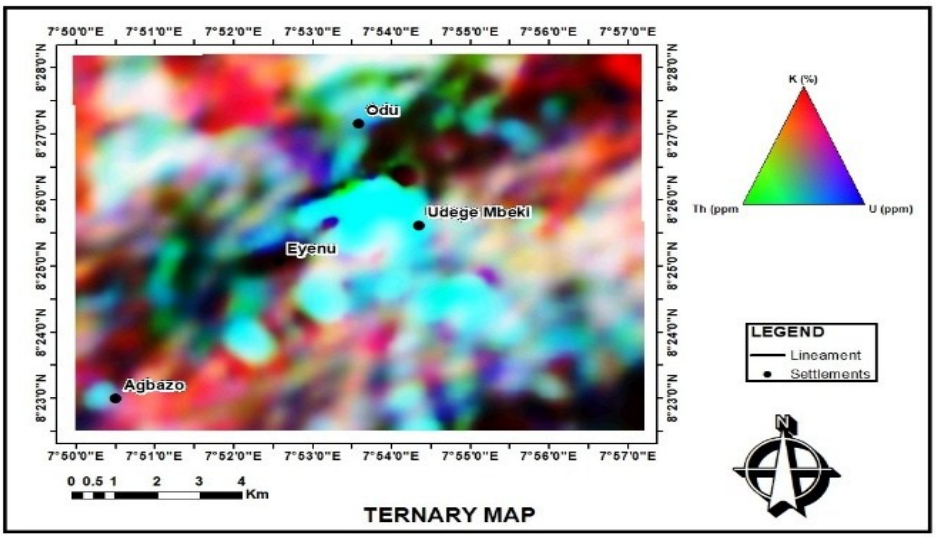

Fig. 13. Ternary map

The rose diagram (Fig. 15) provides a quantitative representation of the orientation frequency of the extracted lineaments and confirms the dominance of the NE–SW to ENE–WSW trends. The secondary E–W orientation suggests the presence of additional structural discontinuities that may represent intersecting fracture systems or subsidiary deformation structures. The identification of these structural orientations is significant because geological lineaments may represent surface expressions of fractures, faults, joints, lithological contacts or other discontinuities within the underlying geological framework (O'Leary et al., 1976).

The reclassified lineament density map (Fig. 16) further illustrates the spatial distribution and concentration of structural features across the study area. The highest lineament densities occur predominantly within the central portion of the complex, coinciding with the NE–SW-trending hydrothermal alteration belt and the principal zones of elevated U/Th ratios. This spatial correspondence suggests that the central structural corridor represents a zone of enhanced structural complexity and potentially increased permeability. Such structural conditions may have facilitated the circulation of hydrothermal fluids and influenced the spatial distribution of secondary mineralization.

Field measurements of fractures and hydrothermal veins indicate predominant orientations between N48°E and N72°E. These measurements are consistent with the dominant NE–SW structural trend obtained from remote sensing and aeromagnetic interpretations. The agreement between remotely extracted lineaments and field-measured structural orientations provides independent support for the interpreted regional structural framework.

The coincidence of elevated lineament density with hydrothermal alteration and radiometric anomalies suggests that the identified

structures may have played an important role in controlling fluid migration and associated mineral redistribution. Nevertheless, lineament orientation and density alone do not establish the kinematics, age or genetic relationship of individual structures with mineralization. Detailed structural measurements, including fracture geometry, cross-cutting relationships, vein orientations and evidence of displacement, are required to establish their tectonic significance.

3.4 Field, Petrographic and Geochemical Validation

Field investigations were conducted to evaluate the geological significance of the remotely sensed alteration zones, radiometric anomalies and interpreted structural features. Field observations identified a prominent NE–SW-trending fracture zone characterized by hydrothermal quartz veins and pegmatitic intrusions. These features occur predominantly within the porphyritic biotite granite (PBG), particularly in the vicinity of the syenite plug. The spatial association of quartz veins and pegmatites with the interpreted structural corridor indicates that the fractures provided potential pathways for the emplacement of late-stage magmatic and hydrothermal fluids.

Some of the observed quartz veins and associated pegmatitic materials contain visible cassiterite crystals (Plate 1). The occurrence of cassiterite provides direct field evidence of tin mineralization and supports the interpretation that the structural corridor experienced mineralizing fluid activity. The association of cassiterite-bearing veins with the fractured granitic host rocks further suggests that structural permeability and late-stage magmatic-hydrothermal processes contributed to the localization of tin mineralization. However, the occurrence of cassiterite does not independently establish the presence of uranium mineralization within the same structures.

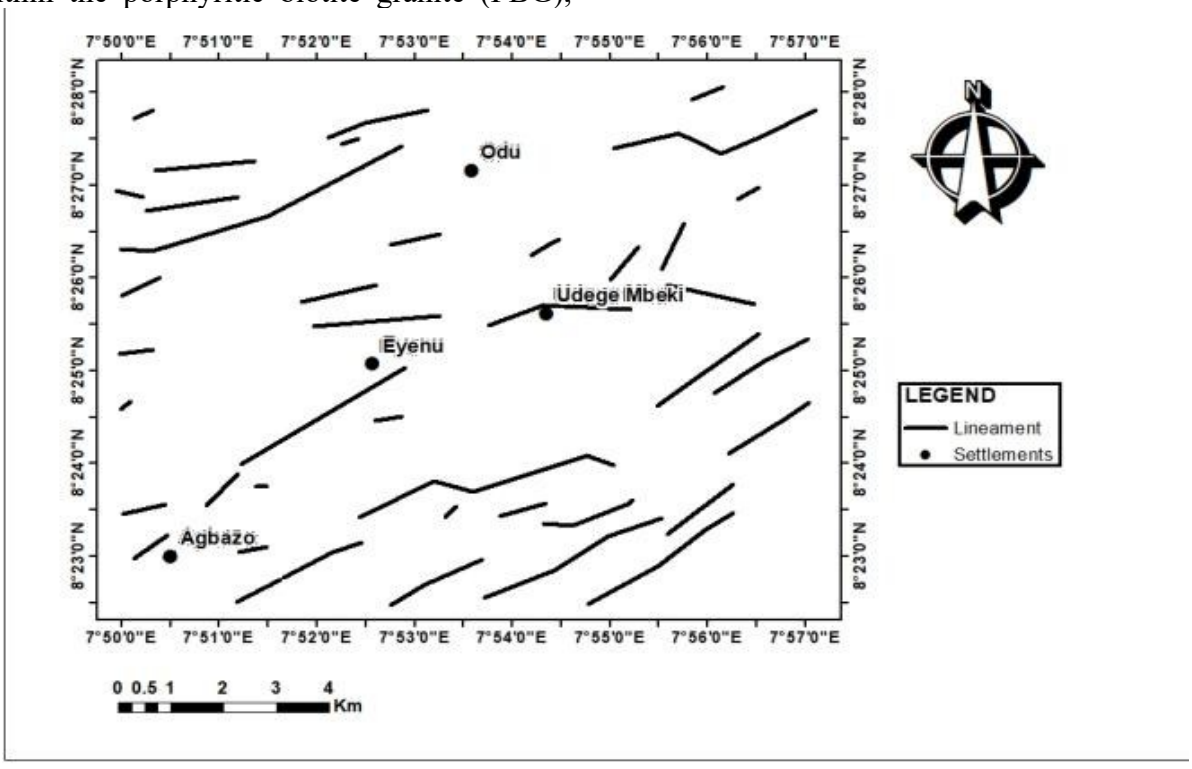

Fig.14 Lineament map

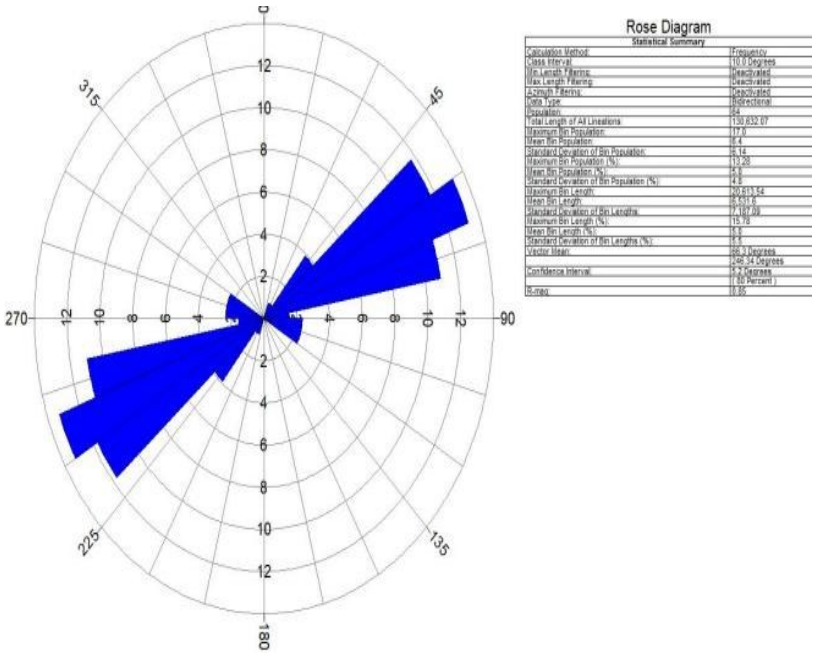

Fig.15: Rose Diagram

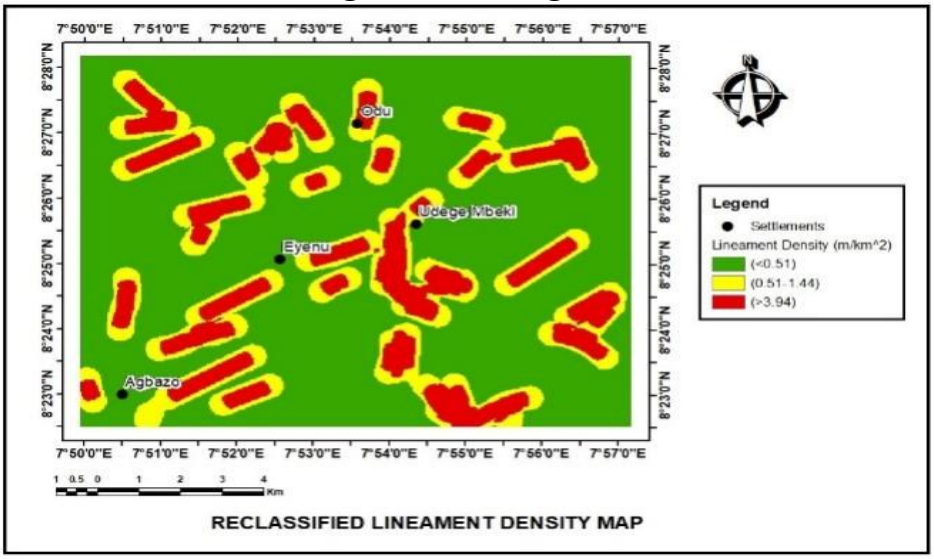

Fig. 16: Reclassified lineament density map

Plate 1. Cassiterite (SnO_2) crystals occurring within porphyritic biotite granite (PBG).

Petrographic examination of samples collected from the identified prospective zones reveals the presence of accessory zircon and monazite, together with mineralogical evidence of hydrothermal alteration. The observed alteration features include sericitization of feldspars and chloritization of biotite. Sericitization is expressed by the development of fine-grained secondary mica within or along feldspar grains, whereas chloritization involves the partial replacement of primary biotite by secondary chlorite. These mineralogical transformations indicate post-magmatic fluid-rock interaction and provide petrographic evidence supporting the hydrothermal

interpretation of the remotely sensed alteration anomalies.

The occurrence of zircon and monazite is particularly relevant to the interpretation of the radiometric signatures because these accessory minerals can accommodate significant quantities of uranium and thorium within their crystal structures. Their presence may therefore contribute to the observed eU and eTh responses. However, the relative contributions of these minerals to the measured radioelement concentrations require mineral-chemical analyses for confirmation.

Geochemical classification using the total alkalis versus silica (TAS) diagram (Fig. 17) indicates that the investigated rocks exhibit alkaline compositional characteristics consistent with the alkaline nature of the Afu Younger Granite Complex. Their classification as A-type granites should, however, be considered in conjunction with diagnostic trace-element characteristics and appropriate geochemical discrimination parameters rather than TAS classification alone.

The primitive mantle-normalized trace-element patterns (Fig. 18), constructed using the normalization values of Sun and McDonough (1989), reveal pronounced positive uranium and thorium anomalies in samples collected from the high-U/Th zones. These enrichments are accompanied by negative anomalies in barium (Ba), strontium (Sr), phosphorus (P) and titanium (Ti). The depletion of Ba and Sr may be associated with feldspar fractionation during magmatic evolution, whereas negative P and Ti anomalies may reflect the fractionation or crystallization of apatite and Ti-bearing accessory minerals, respectively. Such geochemical characteristics are consistent with advanced magmatic differentiation and the development of evolved granitic compositions.

The positive U and Th anomalies indicate enrichment of these elements relative to the primitive mantle reference composition and provide additional evidence of the radioactive-element fertility of the investigated granites. Nevertheless, primitive mantle-normalized enrichment patterns do not independently demonstrate hydrothermal uranium deposition or the presence of economically significant mineralization. Their interpretation is strengthened by the combined evidence from radiometric mapping, structural analysis, petrography and field observations.

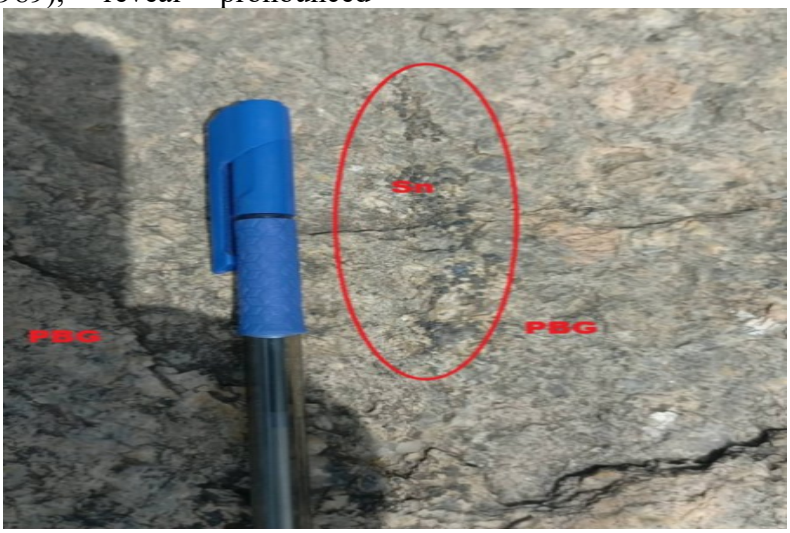

Plate 1 Cassiterite (Sn) crystals in porphyritic biotite granite (PBG).

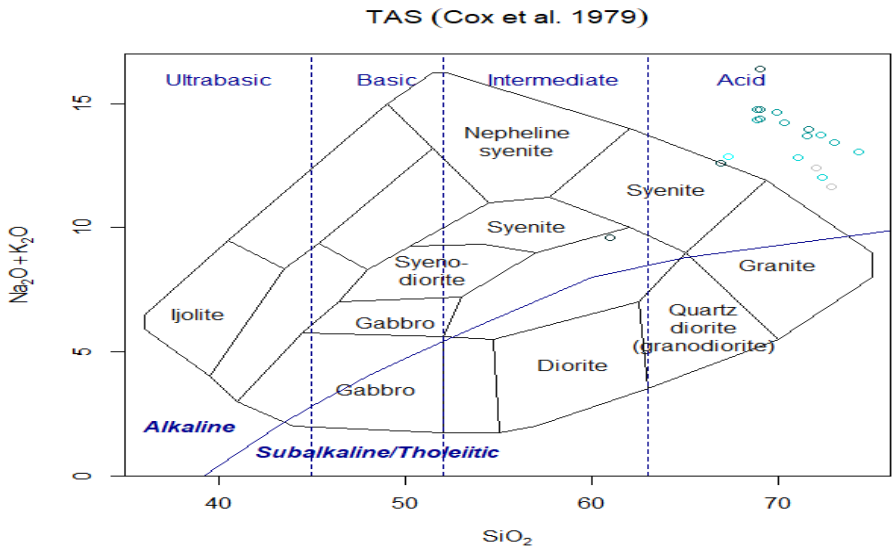

Fig. 17: Total Alkaline vs Silica (TAS)

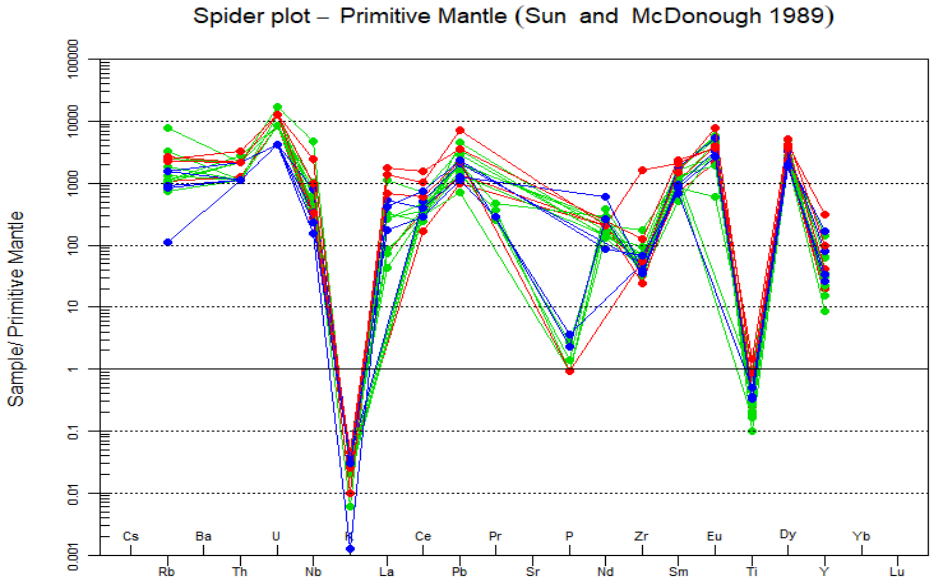

Fig/ 18: Spider Plot-Primitive Mantle (Sun and McDonough 1989)

4.0 Discussion

4.1 Spatial Relationships among Hydrothermal Alteration, Radioelement Distribution and Structural Features

The integrated interpretation of Landsat 8 OLI imagery, airborne radiometric data, aeromagnetic information and field observations reveals a pronounced spatial association among hydrothermal alteration signatures, radioelement anomalies and geological structures within the Afu Younger Granite Complex. The NE–SW-trending alteration belt delineated from the mineral colour composite (Fig. 7) exhibits considerable spatial correspondence with the principal structural corridor identified through lineament extraction and density analysis (Figs. 14 and 16). This relationship indicates that the

alteration distribution is not entirely random but may be associated with structurally controlled fluid circulation within the granitic complex.

Four major geological and geophysical observations support this interpretation. First, the central portion of the study area is characterized by the highest concentration of extracted lineaments, suggesting enhanced structural complexity. Second, the same structural corridor contains localized zones of elevated U/Th ratios, indicating relative uranium enrichment compared with thorium. Third, elevated K/Th ratios occur along portions of the NE–SW trend, suggesting localized variations in potassium abundance that may be related to lithological differences or hydrothermal potassium redistribution. Fourth, field investigations confirm the presence of fractures, hydrothermal quartz veins and pegmatitic bodies, some of which contain visible cassiterite mineralization.

The spatial coincidence of these independent geological observations provides a coherent basis for interpreting the NE–SW structural corridor as a potentially important pathway for magmatic-hydrothermal fluid migration. Fractures and structural discontinuities can increase the permeability of granitic rocks and facilitate the movement of fluids during the late stages of magmatic cooling. Where such structures intersect or develop zones of enhanced fracture density, they may provide favourable conditions for fluid focusing, chemical exchange and mineral precipitation.

The observed relationship between elevated U/Th ratios and the structural corridor is particularly significant. Uranium can be mobilized during hydrothermal processes and subsequently redistributed through fluid-rock interaction, whereas thorium commonly remains comparatively immobile under many of the same geochemical conditions. Consequently, the localized increase in U/Th ratios may reflect uranium enrichment relative to the thorium-bearing mineral background. Nevertheless, variations in lithology, weathering, radioactive disequilibrium and surface redistribution may also influence the observed ratio patterns (IAEA, 2003).

Similarly, the elevated K/Th ratios along the structural corridor may indicate potassium enrichment associated with fluid-rock interaction. However, the presence of K-feldspar-rich granite phases means that primary magmatic composition must also be considered. Petrographic evidence of feldspar sericitization and associated alteration provides support for hydrothermal modification, although the identification of specific potassium-bearing alteration assemblages would require further mineralogical investigation.

The association of hydrothermal quartz veins and cassiterite-bearing pegmatitic bodies with the same structural corridor provides additional evidence of structurally influenced mineralizing activity. These observations suggest that the NE–SW structures played an important role in controlling fluid circulation and the emplacement of at least some late-stage mineralized veins. Similar relationships between structural permeability, hydrothermal alteration and mineralization have been recognized in structurally controlled hydrothermal systems (O'Leary et al., 1976).

Taken together, the integrated results suggest that the central NE–SW structural corridor represents a significant exploration target characterized by the convergence of hydrothermal alteration signatures, elevated relative uranium responses, potassium anomalies and field evidence of mineralizing fluid activity. Although the available data support a structural control on hydrothermal alteration and associated mineralization, direct confirmation of uranium-bearing mineral phases and their spatial relationship with the mapped anomalies requires systematic geochemical and mineralogical investigation.

4.2 Proposed Genetic Model for Radioactive Mineralization in the Afu Complex

Based on the integrated remote sensing, radiometric, structural, petrographic and geochemical observations, a preliminary genetic model is proposed to explain the possible development of uranium enrichment within the Afu Younger Granite Complex (Fig. 19). The model considers the combined influence of magmatic differentiation, structural development, hydrothermal fluid circulation and subsequent uranium redistribution.

The initial stage involved the emplacement and subsequent differentiation of the alkaline A-type granitic magma. Progressive fractional crystallization may have resulted in the enrichment of incompatible elements, including uranium, thorium and rare earth elements, within the residual melt. The geochemical characteristics of the investigated granites, particularly the positive U and Th anomalies and the presence of accessory zircon and monazite, support the interpretation that the granitic rocks possess an inherent capacity to host radioactive elements.

4.2.1 Magmatic Differentiation and Radioelement Enrichment

The enrichment of uranium and thorium during magmatic differentiation would have contributed to the development of a geochemically fertile granitic source. However, their eventual distribution within the crystallized rocks would have depended on the partitioning behaviour of these elements among the major rock-forming minerals, accessory minerals and residual magmatic fluids.

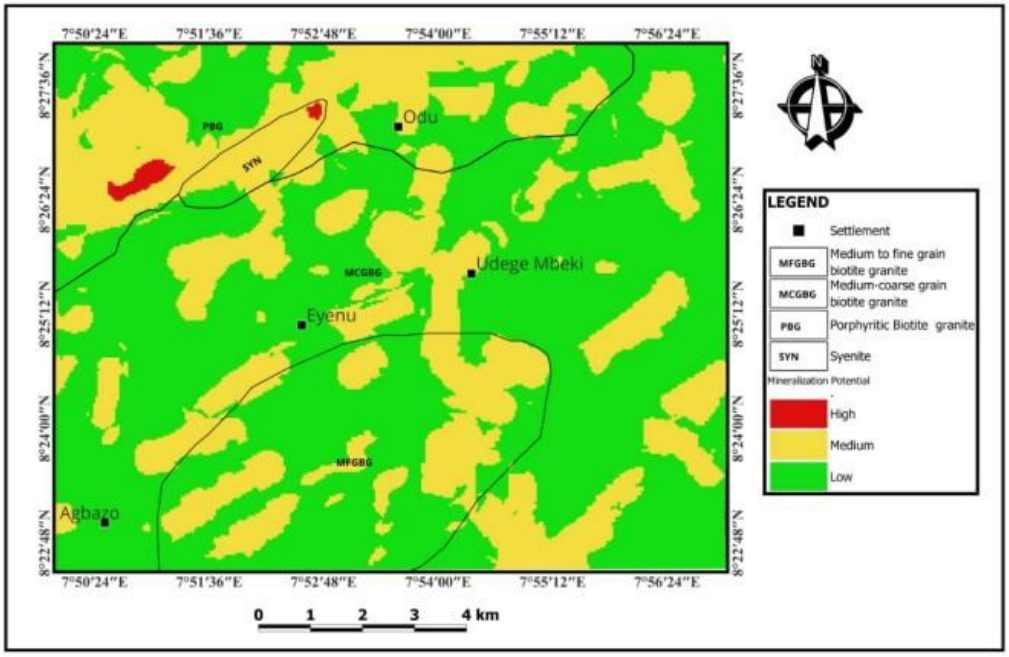

Fig.: 19. integrated map of mineralization potential and geological map

4.2.2 Structural Development and Permeability Enhancement

The second stage involved the development and/or reactivation of the principal NE–SW-trending structural corridor. The structural framework may be related to regional tectonic processes associated with the opening of the South Atlantic and the fragmentation of Gondwana, which influenced the development of extensional structures within parts of West Africa (Burke & Dewey, 1973).

The fractures and structural discontinuities identified in the Afu Complex may have enhanced permeability within the granitic rocks, providing pathways for the migration of late-stage magmatic and hydrothermal fluids. The observed NE–SW and subordinate E–W structural orientations suggest the development of a fracture network capable of facilitating localized fluid circulation.

Although the regional tectonic framework provides a plausible context for structural development, the available structural data do not independently establish the age or kinematic history of the mapped lineaments. Detailed structural and geochronological investigations would be necessary to establish their precise tectonic relationship with the emplacement and mineralization history of the complex.

4.2.3 Hydrothermal Fluid Circulation and Rock Alteration

During the late stages of magmatic crystallization, residual fluids enriched in volatile components and incompatible elements may have separated from the crystallizing granitic system. These fluids could have migrated through the structurally permeable NE–SW corridor, interacting with the surrounding granitic rocks and producing localized hydrothermal alteration.

The observed sericitization of feldspars, chloritization of biotite and development of hydrothermal quartz veins provide petrographic evidence of fluid-rock interaction. The corresponding Landsat-derived alteration anomalies and localized radiometric variations further support the interpretation of a structurally influenced hydrothermal system.

The occurrence of cassiterite-bearing veins and pegmatitic bodies indicates that the hydrothermal system was also associated with the redistribution and concentration of tin and other incompatible elements. The presence of potassium-rich radiometric responses may reflect potassium redistribution during alteration, although primary magmatic mineralogical variations may also have contributed to the observed patterns.

4.2.4 Uranium Mobilization and Possible Secondary Deposition

The final stage of the proposed model involves the possible mobilization and redistribution of uranium by hydrothermal fluids. Under oxidizing conditions, uranium may be transported in aqueous solutions as soluble uranyl complexes, particularly where carbonate or other suitable complexing ligands are present. Changes in fluid chemistry, redox conditions, temperature, pressure and fluid-rock interaction may subsequently promote uranium precipitation within structurally favourable environments.

Potential sites of uranium accumulation include fracture intersections, vein systems, fault-related breccias and zones characterized by favourable chemical conditions. The comparatively immobile behaviour of thorium under many near-surface geochemical conditions may have contributed to the development of localized areas with elevated U/Th ratios.

The coincidence of high U/Th anomalies, hydrothermal alteration signatures and structural concentrations along the central NE–SW corridor is consistent with this proposed process. However, the available results do not establish the occurrence of specific uranium minerals such as uraninite or coffinite. Their presence remains a hypothesis that requires confirmation through detailed mineralogical investigations, including scanning electron microscopy (SEM), energy-dispersive X-ray spectroscopy (EDS) and electron probe microanalysis (EPMA).

The proposed model therefore provides a testable geological explanation for the observed spatial association between magmatic fertility, hydrothermal alteration, structural

permeability and relative uranium enrichment within the Afu Younger Granite Complex.

4.3 Implications for Mineral Exploration

The integrated results have important implications for radioactive and rare-metal mineral exploration within the Afu Younger Granite Complex and comparable granitic terrains. The combined interpretation of multispectral remote sensing, airborne gamma-ray spectrometry, aeromagnetic data and field observations demonstrates the value of integrating complementary geological and geophysical datasets for regional exploration targeting.

4.3.1 Application of Integrated Geospatial Techniques

The integration of Landsat 8 OLI imagery and airborne radiometric data provides an effective reconnaissance-level exploration approach for delineating lithological variations, hydrothermal alteration signatures and radioelement anomalies over relatively extensive areas. The application of band ratios, PCA and radiometric ratio analysis facilitates the identification of prospective geological environments that may not be readily distinguishable through conventional geological mapping alone.

The incorporation of aeromagnetic data further improves structural interpretation by providing information on subsurface magnetic contrasts and possible geological discontinuities. This integrated approach can reduce the spatial extent requiring detailed ground investigation and improve the prioritization of exploration targets, particularly in areas with difficult terrain or limited geological accessibility.

4.3.2 Identification and Prioritization of Prospective Zones

The central NE–SW structural corridor represents the most significant exploration target identified in this study. Its prospectivity is supported by the convergence of several geological and geophysical indicators, including:

- Elevated U/Th ratios, indicating relative uranium enrichment.
- Localized potassium and K/Th anomalies, potentially associated with hydrothermal alteration.
- Landsat-derived spectral signatures interpreted as iron oxide-, hydroxyl- and clay-bearing alteration zones.
- High lineament density, suggesting enhanced structural complexity and potential fluid pathways.
- Field occurrences of hydrothermal quartz veins, pegmatites and visible cassiterite mineralization.
- Petrographic evidence of sericitization, chloritization and the presence of zircon and monazite.

The coincidence of these features provides a rational basis for prioritizing the central structural corridor for detailed follow-up exploration. Nevertheless, the anomalies should be regarded as prospective targets rather than confirmed uranium mineral deposits until supported by direct geochemical and mineralogical evidence.

4.3.3 Development of a Predictive Exploration Framework

The spatial relationship between hydrothermal alteration, structural lineaments and radiometric anomalies provides a preliminary predictive framework for identifying additional exploration targets within the Afu Complex. In particular, other NE–SW-trending structural segments exhibiting similar alteration signatures, elevated U/Th ratios and high lineament densities may warrant further investigation.

The proposed framework can be adapted to other evolved granitic environments where rare-metal and radioactive mineralization is associated with structural discontinuities and hydrothermal alteration. Its application should,

however, incorporate local geological controls, lithological variations and surface-cover characteristics to avoid interpreting all radiometric or spectral anomalies as mineralization indicators.

4.4 Limitations of the Study and Recommendations for Future Investigations

Although the integration of remote sensing, airborne radiometric and structural datasets provides useful information for regional mineral exploration, the approach is subject to certain limitations. Landsat 8 OLI imagery primarily characterizes surface spectral properties and may not adequately resolve alteration beneath vegetation, soil cover or transported regolith. Similarly, airborne gamma-ray spectrometry principally reflects radioelement concentrations within the near-surface environment and cannot independently establish the depth, geometry or grade of concealed mineralization. In addition, equivalent uranium concentrations may differ from actual chemical uranium concentrations where radioactive disequilibrium occurs within the uranium decay series (IAEA, 2003).

The present investigation therefore provides a regional-scale delineation of prospective alteration and radiometric anomaly zones rather than a definitive assessment of uranium deposit geometry or economic viability. Further investigations are necessary to establish the continuity, depth extent, mineralogical composition and geochemical characteristics of the identified targets.

The following investigations are recommended:

4.4.1 Detailed Ground Geophysical Surveys

Ground-based magnetic and radiometric surveys should be conducted along the principal NE–SW structural corridor to verify the airborne anomalies and improve the spatial resolution of the identified targets. Induced polarization (IP) and electrical resistivity surveys may also be employed to investigate subsurface structural features, alteration zones and possible mineralized vein systems. The selection of these methods should be guided by the expected mineralization style and the physical properties of the target rocks.

4.4.2 Systematic Geochemical Sampling

A systematic geochemical sampling programme should be undertaken across the identified radiometric and alteration anomalies. Soil, stream-sediment and representative rock-chip samples should be collected along and across the principal structural corridor to establish the spatial distribution of uranium, thorium and associated pathfinder elements. Laboratory analyses should include U, Th, Sn, W, Nb, Ta and relevant rare earth elements, depending on the mineralization model. Particular attention should be given to determining whether the elevated airborne eU responses correspond to actual chemical uranium enrichment.

4.4.3 Detailed Mineralogical and Petrographic Investigations

Further mineralogical investigations should be conducted to determine the specific radioactive and accessory mineral phases associated with the identified prospective zones. Scanning electron microscopy, energy-dispersive X-ray spectroscopy and electron probe microanalysis would be useful for identifying uranium- and thorium-bearing minerals and establishing their textural relationships with zircon, monazite, cassiterite and other accessory phases. These investigations would also help distinguish primary magmatic mineralization from secondary hydrothermal mineral deposition.

4.4.4 Targeted Drilling and Subsurface Evaluation

Following the confirmation of surface and near-surface geochemical anomalies, targeted drilling should be undertaken to evaluate the subsurface continuity and geometry of the prospective structures. Drill-core logging, downhole radiometric measurements and

laboratory geochemical analyses would provide essential information on mineralization thickness, grade distribution, structural orientation and alteration intensity. The results would establish whether the identified radiometric anomalies represent significant subsurface uranium mineralization and provide the basis for subsequent resource evaluation.

5.0 Conclusions

This study integrated Landsat 8 Operational Land Imager (OLI) imagery, airborne radiometric data, aeromagnetic information and field-based geological observations to investigate hydrothermal alteration zones and structural controls on potential radioactive mineralization within the Afu Younger Granite Complex, Nigeria. The results demonstrate the effectiveness of combining multispectral remote sensing, airborne gamma-ray spectrometry and structural analysis for delineating prospective mineralized zones in evolved granitic terrains.

The remote sensing analysis, particularly false colour composite, band ratios and Principal Component Analysis, revealed distinct lithological variations and a prominent NE–SW-trending hydrothermal alteration belt across the central part of the study area. The airborne radiometric results further identified significant variations in potassium, equivalent uranium and equivalent thorium concentrations. Potassium concentrations ranged from −0.3% to 3.6%, eTh from 14.3 to 88.2 ppm, and eU from 3.8 to 20.1 ppm. Notably, elevated U/Th ratios exceeding 4.5 were concentrated predominantly along the central NE–SW structural corridor, suggesting localized relative uranium enrichment. The spatial distribution of these anomalies, together with elevated K/Th responses, provides important evidence of possible hydrothermal modification and radioelement redistribution within the complex.

Structural analysis established the dominance of NE–SW to ENE–WSW-trending lineaments, with subordinate E–W orientations. The highest lineament densities coincide spatially with the principal alteration belt and elevated U/Th anomalies. Field measurements of fractures and veins, predominantly oriented between N48°E and N72°E, further support the interpreted structural framework. Field investigations also confirmed the occurrence of hydrothermal quartz veins, pegmatites and cassiterite-bearing mineralized structures within the porphyritic biotite granite, providing evidence of structurally influenced hydrothermal activity. Petrographic observations of feldspar sericitization, biotite chloritization, zircon and monazite, together with the geochemical characteristics of the investigated granites, further indicate magmatic differentiation and subsequent hydrothermal modification.

The integrated evidence suggests that the central NE–SW-trending structural corridor played an important role in controlling hydrothermal fluid circulation and the distribution of alteration and radioelement anomalies. The observed uranium-to-thorium ratio anomalies are consistent with possible preferential uranium redistribution and enrichment relative to thorium. However, the presence of economically significant uranium mineralization and specific uranium-bearing mineral phases has not yet been established and requires further geochemical and mineralogical confirmation.

This study establishes an integrated geospatial exploration framework for identifying prospective radioactive and associated rare-metal mineralization in the Afu Younger Granite Complex. The convergence of hydrothermal alteration signatures, structural complexity, radiometric anomalies and field evidence provides a rational basis for prioritizing the central NE–SW structural corridor for detailed exploration. Further ground radiometric surveys, systematic geochemical sampling, mineralogical

characterization and targeted drilling are recommended to establish the depth extent, mineralogical composition and economic significance of the identified anomalies. The methodology also offers a potentially cost-effective approach for preliminary mineral exploration in comparable granitic terrains within Nigeria and elsewhere.

6.0 References

Adiri, Z., Lhissou, R., El Harti, A., Jellouli, A., & Chakouri, M. (2020). Recent advances in the use of public domain satellite imagery for mineral exploration: A review of Landsat-8 and Sentinel-2 applications. *Ore Geology Reviews,* 117, Article 103332. https://doi.org/10.1016/j.oregeorev.2020.103332

Amuda, A. K., Yang, X. Y., Deng, J., et al. (2020). Petrogenesis of the peralkaline Dutsen Wai and Ropp complexes in the Nigerian Younger Granites: Implications for crucial metal enrichments. *International Geology Review,* 63, 16, pp, 2057–2081.

Bowden, P., Kinnaird, J. A., & Whitley, J. E. (1987). *The Younger Granites of Nigeria: A study of anorogenic alkaline granites*. Geological Society of London.

Burke, K., & Dewey, J. F. (1973). Plume-generated triple junctions: Key indicators in applying plate tectonics to old rocks. *The Journal of Geology,* 81, 4, pp. 406–433. https://doi.org/10.1086/627882

Chattoraj, S. L., Prasad, G., Sharma, R. U., Champati Ray, P. K., van der Meer, F. D., Guha, A., & Beiranvand Pour, A. (2020). Integration of remote sensing, gravity and geochemical data for exploration of Cu-mineralization in Alwar basin, Rajasthan, India. *International Journal of Applied Earth Observation and Geoinformation, 91*, Article 102162. https://doi.org/10.1016/j.jag.2020.102162

Dickson, B. L., & Scott, K. M. (1997). Interpretation of airborne gamma-ray spectrometric data for geological mapping. *Journal of Geochemical Exploration,* 58, 1, pp. 1–18.

Erdi-Krausz, G., Matolin, M., Minty, B., Nicolet, J. P., Reford, W. S., & Schetselaar, E. M. (2003). *Guidelines for radioelement mapping using gamma ray spectrometry data* (IAEA-TECDOC-1363). International Atomic Energy Agency.

Fotze, Q. M. A., Lordon, A. E. D., Penaye, J., Sep, J. P., & Fru, M. I. N. (2019). Mapping hydrothermal alteration targets from Landsat 8 OLI/TIRS and magnetic data using digital image processing techniques in Garoua, North Cameroon. *Journal of Geosciences and Geomatics,* 7, 1, pp. 28–41. https://doi.org/10.12691/jgg-7-1-4

Girei, M. B., Li, H., Algeo, T. J., Bonin, B., Ogunleye, P. O., Bute, S. I., & Ahmed, H. A. (2019). Petrogenesis of A-type granites associated with Sn–Nb–Zn mineralization in Ririwai complex, north-central Nigeria: Constraints from whole-rock Sm–Nd and zircon Lu–Hf isotope systematics. *Lithos,* 340–341, pp. 49–70. https://doi.org/10.1016/j.lithos.2019.05.003

Imeokparia, E. G. (1981). Ba/Rb and Rb/Sr ratios as indicators of magmatic fractionation, postmagmatic alteration and mineralization—Afu Younger Granite Complex, northern Nigeria. *Geochemical Journal,* 15, 4, pp. 209–219.

Imeokparia, E. G. (1982). Geochemistry and relationships to mineralization of granitic rocks from the Afu Younger Granite Complex, central Nigeria. *Geological Magazine,* 119, 1, pp. 39–56.

International Atomic Energy Agency. (2003). *Guidelines for radioelement mapping using gamma ray spectrometry data* (IAEA-TECDOC-1363). https://www.iaea.org/publications/6749/guidelines-for-radioelement-mapping-using-gamma-ray-spectrometry-data

Jacobson, R. R. E., MacLeod, W. N., & Black, R. (1958). *Ring complexes in the Younger Granite Province of northern Nigeria* (Geological Survey of Nigeria Memoir No. 1).

Kinnaird, J. A., Bowden, P., & Ixer, R. A. (1985). Mineralization in the Younger Granites of Nigeria. *Economic Geology, 80*(4), 857–874.

Loughlin, W. P. (1991). Principal component analysis for alteration mapping. *Photogrammetric Engineering & Remote Sensing, 57*(9), 1163–1169.

Moxham, R. M., Foote, R. S., & Bunker, C. M. (1965). Gamma-ray spectrometer studies of hydro-thermally altered rocks. *Economic Geology, 60*(4), 653–671. https://doi.org/10.2113/gsecongeo.60.4.653

O'Leary, D. W., Friedman, J. D., & Pohn, H. A. (1976). Lineament, linear, lineation: Some proposed new standards for old terms. *Geological Society of America Bulletin, 87*(10), 1463–1469. https://doi.org/10.1130/0016-7606(1976)87%3C1463:LLLSPN%3E2.0.CO;2

Rowan, L. C., Mars, J. C., & Simpson, C. J. (2003). Lithologic mapping in the Mountain Pass, California area using Advanced Spaceborne Thermal Emission and Reflection Radiometer (ASTER) data. *Remote Sensing of Environment, 84*(3), 350–366.

Sabins, F. F. (1999). Remote sensing for mineral exploration. *Ore Geology Reviews, 14*(3–4), 157–183.

Sun, S.-S., & McDonough, W. F. (1989). Chemical and isotopic systematics of oceanic basalts: Implications for mantle composition and processes. In A. D. Saunders & M. J. Norry (Eds.), *Magmatism in the ocean basins* (Geological Society, London, Special Publications, Vol. 42, pp. 313–345). Geological Society of London. https://doi.org/10.1144/GSL.SP.1989.042.01.19

Whalen, J. B., Currie, K. L., & Chappell, B. W. (1987). A-type granites: Geochemical characteristics, discrimination and petrogenesis. *Contributions to Mineralogy and Petrology, 95*(4), 407–419.

Wilford, J. R., Bierwirth, P. N., & Craig, M. A. (1997). Application of airborne gamma-ray spectrometry in soil/regolith mapping and environmental monitoring. *Journal of Australian Geology & Geophysics, 17*(2), 201–216.

Yang, C., Jia, H., Dong, L., Zhao, H., & Zhao, M. (2024). Selection of Landsat-8 Operational Land Imager (OLI) optimal band combinations for mapping alteration zones. *Remote Sensing, 16*(2), Article 392. https://doi.org/10.3390/rs16020392

Acknowledgements

The authors are grateful to the Nigerian Geological Survey Agency (NGSA) for providing the aeromagnetic and aeroradiometric data. We also acknowledge the USGS for free access to Landsat data. Special thanks to Abdulgaffar Okkoh for his support during fieldwork.

Declarations

Ethical Approval and Consent to Participate

Bot applicab;e

Availability of Data and Materials

Data shall be made available upon request

Competing Interests

The authors declare that they have no competing interests.

Funding

The authors declared no source of funding

Author Contributions

Both authors were involved in drafting the original manuscript based on the work that was designed by the first author. The two authors were equally involved in all other steps,